Atmos. Chem. Phys., 24, 13101–13113, 2024
https://doi.org/10.5194/acp-24-13101-2024

Atmospheric Chemistry and Physics
Open Access
EGU

Research article

Development of a high-spatial-resolution annual emission inventory of greenhouse gases from open straw burning in Northeast China from 2001 to 2020

Zihan Song[1,2], Leiming Zhang[3], Chongguo Tian[4], Qiang Fu[1,2], Zhenxing Shen[5], Renjian Zhang[6], Dong Liu[1,2], and Song Cui[1,2]

[1]International Joint Research Center for Persistent Toxic Substances (IJRC-PTS), School of Water Conservancy and Civil Engineering, Northeast Agricultural University, Harbin, Heilongjiang, 150030, China
[2]Research Center for Eco-Environment Protection of Songhua River Basin, Northeast Agricultural University, Harbin, Heilongjiang, 150030, China
[3]Air Quality Research Division, Science and Technology Branch, Environment and Climate Change Canada, Toronto, Ontario, M3H 5T4, Canada
[4]CAS Key Laboratory of Coastal Environmental Processes and Ecological Remediation, Yantai Institute of Coastal Zone Research, Chinese Academy of Sciences, Shandong Key Laboratory of Coastal Environmental Processes, YICCAS, Yantai, 264003, China
[5]Department of Environmental Sciences and Engineering, Xi'an Jiaotong University, Xi'an, 710049, China
[6]Institute of Atmospheric Physics, Chinese Academy of Sciences, Beijing, 100029, China

Correspondence: Song Cui (cuisong-bq@neau.edu.cn)

Received: 1 April 2024 – Discussion started: 3 May 2024
Revised: 30 September 2024 – Accepted: 30 September 2024 – Published: 27 November 2024

Abstract. Open straw burning has been widely recognized as a significant source of greenhouse gases (GHGs), posing critical risks to atmospheric integrity and potentially exacerbating global warming. In this study, we proposed a novel method that integrates crop cycle information into extraction and classification of fire spots from open straw burning in Northeast China from 2001 to 2020. By synergizing the extracted fire spots with the modified fire radiative power (FRP) algorithm, we developed high-spatial-resolution emission inventories of GHGs, including carbon dioxide (CO_2), methane (CH_4), and nitrous oxide (N_2O). Results showed that the northern Sanjiang Plain, eastern Songnen Plain, and eastern Liao River plain were areas with high intensity of open straw burning. The number of fire spots was evaluated during 2013–2017, accounting for 58.2 % of the total fire spots observed during 2001–2020. The prevalent season for open straw burning shifted from autumn (pre-2016) to spring (post-2016), accompanied by a more dispersed pattern in burning dates. The 2-decade cumulative emissions of CO_2, CH_4, and N_2O were quantified at 198 Tg, 557 Gg, and 15.7 Gg, respectively, amounting to 218 Tg of CO_2-eq (equivalent). Significant correlations were identified between GHG emissions and both straw yield and straw utilization ($p < 0.01$). The enforcement of straw-burning bans since 2018 has played a pivotal role in curbing open straw burning and has reduced fire spots by 51.7 % on an annual basis compared to 2013–2017. The novel method proposed in this study considerably enhanced the accuracy in characterizing spatiotemporal distributions of fire spots from open straw burning and quantifying associated pollutant emissions.

Published by Copernicus Publications on behalf of the European Geosciences Union.

1 Introduction

Open straw burning, a customary practice in agricultural areas, serves multiple purposes, including rapid straw disposal, weed control, nutrient release, and pest management (Korontzi et al., 2006; Wen et al., 2020). This practice results in short-term yet intense emissions of greenhouse gases (GHGs), such as carbon dioxide (CO_2), methane (CH_4), and nitrous oxide (N_2O). The accumulation of these gases in the atmosphere adversely impacts climate and atmospheric chemistry (Weldemichael and Assefa, 2016; Tang et al., 2020; Hong et al., 2023). To date, open straw burning remains prevalent in grain-producing areas globally, despite the many drawbacks of such a practice (Gadde et al., 2009; Huang et al., 2013; Zhu et al., 2015; Ahmed et al., 2019; Mehmood et al., 2020; Fu et al., 2022; Huang et al., 2023; Xu et al., 2023). Thus, accurate and high-spatial-resolution emission inventories for GHGs from this source sector are needed from regional to global scales to assess potential climate and air quality impacts and formulate carbon mitigation policies.

The "bottom-up" approach, which is based on the amount of straw burned and corresponding emission factors, has been widely employed to establish emission inventories for various pollutants emitted from open straw burning (van der Werf et al., 2017; Wang et al., 2018; Liu et al., 2021; Zheng et al., 2023). Emission factors for diverse pollutants released from different types of straw burning have been extensively investigated in laboratory studies (Li et al., 2007; Liu et al., 2011; Stockwell et al., 2014; Pan et al., 2017; Peng et al., 2016; Sun et al., 2016). However, estimation of the amount of straw burned is subject to large uncertainties since it involves many parameters, such as grain yield, ratio of straw and grain, open burning proportion, burning efficiency, and dry matter fraction (Guan et al., 2017; Zhou et al., 2017). Consequently, existing regional-scale emission inventories based on the "bottom-up" approach generally have large uncertainties and low spatiotemporal resolutions (Tian et al., 2011; Jin et al., 2017).

The advent of satellite technologies, such as the Moderate Resolution Imaging Spectroradiometer (MODIS, remote sensing instrument), Visible Infrared Imaging Radiometer Suite (VIIRS, remote sensing instrument), and Himawari-8 (geostationary satellite), has markedly revolutionized the monitoring of open straw burning, enabling real-time and high-spatiotemporal-resolution fire spot products to be accessible to the general public (Schroeder et al., 2014; Giglio et al., 2016; Xu et al., 2017; Wu et al., 2018; Zhuang et al., 2018; Lv et al., 2024). Many studies have effectively utilized satellite fire spot products for constructing emission inventories, based on either the burned area (BA) or fire spot counts (FCs) (Ke et al., 2019; Cui et al., 2021). Several studies have also developed a hybrid inventory strategy using the "bottom-up" approach to allocate GHG emissions spatially and temporally based on BA or FCs (Huang et al., 2012; Jin et al., 2018; Zhang et al., 2019; Kumar et al., 2021). These approaches have significantly improved the spatiotemporal resolutions of the emission inventories for open straw burning (Wu et al., 2023).

MODIS and VIIRS, both operating in polar orbits, provide only two observations per day. MODIS has provided 1 km resolution fire data since 2000, which are suitable for long-term trend analyses (Chen et al., 2022), while VIIRS has provided fire data at a 375 m resolution since 2012, which is more suitable for detecting small fires (Chen et al., 2022). Himawari-8 (geostationary orbit) has provided 10 min temporal resolution and 2 km spatial resolution fire data since 2015, ideal for real-time monitoring across the Asia–Pacific region (Zhang et al., 2020). However, the aforementioned datasets remain inadequate for accurately capturing small-area, short-duration open straw burning, particularly in scattered farmlands (Wiedinmyer et al., 2014). It should also be noted that meteorological disturbances, such as cloud cover and rainfall, can reduce the accuracy of these products (Schroeder et al., 2014; Ying et al., 2019). Furthermore, straw burning during non-satellite transit periods, on cloudy days, at night, and under heavy haze may not be captured in these datasets (Liu et al., 2020). For example, Liu et al. (2019) found that same-day omission error of MODIS burned area product could be as high as 95 % for agricultural fire detection during the post-monsoon season in northwestern India.

With continuous enrichment of satellite data, a strong relationship was observed between fire radiative power (FRP) and emission amounts from open straw burning (Wu et al., 2023). Consequently, the FRP algorithm has been widely accepted for estimating emissions (Wooster et al., 2005; Freeborn et al., 2008; Vermote et al., 2009; Yang and Zhao, 2019). The FRP algorithm has been optimized by integrating multi-source satellite fire spot data, field survey data, and ground observation data and combined with advanced modeling techniques to improve the accuracy of emission inventory for open straw burning. For example, Liu et al. (2020) revised FRP by combining household survey results with satellite observations in northern India to capture small fires, fill cloud/haze gaps in satellite observations, and adjust partial-field burns and diurnal cycle of fire activity disturbances. Yang et al. (2020) improved the FRP algorithm by calibrating the contributions of open straw burning to ground observation data in Northeast China based on model simulation results using the coupled Weather Research and Forecast-

ing model and Community Multiscale Air Quality (WRF-CMAQ) model.

At present, the identification of straw types in open straw burning typically relies on crop data, such as the International Geosphere-Biosphere Programme (IGBP)-Modified MODIS Land Use and MapSPAM datasets (Ke et al., 2019; Yang et al., 2020). These low-spatiotemporal-resolution crop data contribute to errors in both the extraction of fire spots and the identification of straw types (Ke et al., 2019; Liu et al., 2022). Additional errors come from planting structure adjustment and frequent variations in crop phenology. For instance, fire spots that occurred during crop growth might be incorrectly classified as open straw burning, while those that occurred prior to crop growth could be inaccurately attributed to burning of straw from subsequent harvests (Zhou et al., 2022). Therefore, high-spatiotemporal-resolution data on crop types and phenology are critical, and such data should be integrated into the extraction and classification of fire spots from open straw burning to accurately estimate emissions of various pollutants from this source sector.

To control emissions from open straw burning, the Air Pollution Prevention and Control Action Plan (APPCAP) went into effect in 2013 in China (Huang et al., 2021). In addition, China committed to achieving a carbon peak by 2030 and carbon neutrality by 2060, which draws unprecedented challenges in reducing carbon emissions from open straw burning (Wu et al., 2023). As a significant grain-producing region in China, Northeast China produced 1.35×10^8 t of major grains (corn, rice, beans, and wheat) in 2020, accounting for 21.4 % of total production in China (National Bureau of Statistics of China, 2021). During 2013–2018, open straw burning in Northeast China exhibited an increasing trend while decreasing in all other regions of China (Huang et al., 2021). The constant increase reflects the expansion of the agricultural sector and economic development in Northeast China yet relatively unconstrained open burning activities (Huang et al., 2021). Liu et al. (2022) estimated CO_2 emissions from open straw burning in Northeast China to be as high as 344 Tg from 2012 to 2020.

In this study, high-spatial-resolution fire spot products were used to develop annual emission inventories of GHGs, including CO_2, CH_4, and N_2O, from open straw burning in Northeast China for the period of 2001–2020. To improve the accuracy of the developed emission inventory, a novel concept that integrates the crop cycle information into fire spot extraction and classification was adopted. Furthermore, this study conducted a thorough analysis to assess the driving factors influencing GHG emissions during the 2 decades. This study comprehensively examined GHG emissions from open straw burning in Northeast China and offered valuable insights for policy makers to mitigate carbon emissions and air pollution in agricultural areas.

2 Methodology

2.1 Extraction and classification of fire spots

The MODIS fire product (MCD14ML, Collection 6.1) was selected from 1 January 2001 to 31 December 2020 for the whole region of Northeast China (Giglio et al., 2016, https://sftp://fuoco.geog.umd.edu, last access: 4 July 2024). The dataset, with a spatial resolution of about 1 km^2, includes essential variables, such as latitude, longitude, acquisition date and time (in UTC), satellite (Aqua or Terra), FRP, and fire type (presumably vegetation fire, active volcano, other static land source, and offshore), among others (https://modis-fire.umd.edu/files/MODIS_C6_C6.1_Fire_User_Guide_1.0.pdf, last access: 4 July 2024). Non-vegetation fire activities (active volcano, other static land source, and offshore) were then filtered out from the selected dataset for subsequent analysis.

To clarify, the MCD14ML underestimated fire spots in 2001 and 2002 because only the Terra satellite was operational before 3 July 2002. Therefore, data for the years 2003 to 2020 were used for developing annual emission inventories, with relevant results for 2001 and 2002 as reference only. Also, failure of the Aqua satellite on 16 August 2020 led to the loss of fire spot data for about 2 weeks (https://modis-fire.umd.edu/files/MODIS_C61_BA_User_Guide_1.1.pdf, last access: 4 July 2024). However, as August is a crop-growing period in Northeast China, this failure would not lead to an underestimation of fire spots from open straw burning.

The ChinaCropArea1 km and ChinaCropPhen1 km datasets were used to extract and classify fire spots from open straw burning (Luo et al., 2020a, b). These datasets present annual data on the type and phenology (day of year (DOY) of emergence and maturity) of grain crops (corn, rice, and wheat). Considering that Northeast China is a major bean-producing area, we also compiled bean distribution datasets (Li et al., 2021; Xuan et al., 2023). However, bean distribution in Jilin and Liaoning provinces was not recorded during 2001–2012 in this dataset. The dataset was extended to the whole region of Northeast China (Heilongjiang, Jilin, and Liaoning provinces) after 2013. Thus, some gaps still exist in these datasets compared to the comprehensive information required for this study, as detailed in Table S1 in the Supplement.

Figure 1 describes the meticulous process of accurately extracting and classifying fire spots from open straw burning in areas experiencing one harvest season every year. The process involves several key steps:

> In Step 1, the current year's ChinaCropPhen1 km and ChinaCropArea1 km data, along with the previous year's ChinaCropArea1 km data, were extracted to fire spots (MCD14ML) by ArcGIS 10.2 software to obtain the Fire spots–Crop–Phen dataset.

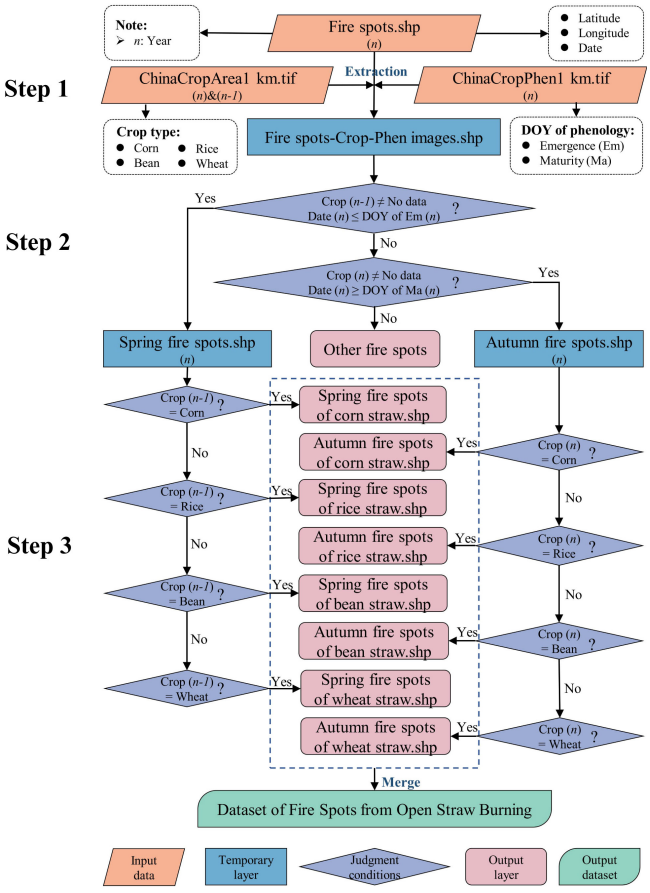

Figure 1. Extraction and classification method for fire spots from open straw burning.

In Step 2, considering the crop cycle, the extraction of fire spots was divided into two stages. The first stage is before crop growth (spring) and requires the fire spot to satisfy two conditions: (a) there was a crop planted in the previous year, and (b) the burning date is before emergence. The second stage is after crop growth (autumn) and also involves two conditions: (a) there was a crop planted in the current year, and (b) the burning date is after maturity.

In Step 3, for fire spots in spring, the type of straw burned is identified based on the previous year's crop type. For autumn fire spots, the straw type is determined according to the crop type of the current year.

Furthermore, fire spots from open straw burning were extracted using the traditional method that does not integrate crop cycle information. Only the current year's ChinaCropArea1 km data were extracted to fire spots (MCD14ML). Then, fire spots occurring on agricultural land with growing crops were identified as open straw burning.

Table 1. Emission factors of open straw burning for different crop types.

Crop	Emission factors ($g\,kg^{-1}$)		
	CO_2	CH_4	N_2O
Corn	1350	4.4	0.12
Rice	1460	3.2	0.11
Bean	1445	3.9	0.09
Wheat	1460	3.4	0.05

2.2 Development of high-spatial-resolution annual emission inventories for GHGs and exploration of driving factors

Annual emission inventories for GHGs were developed for the region of Northeast China at a grid resolution of 5 km × 5 km for the years 2001 to 2020. The domain grids were created using Fishnet of ArcGIS 10.2 software.

The modified FRP algorithm (Yang et al., 2020) is used to estimate the emissions of GHGs from open straw burning in this study:

$$E = \alpha \times \int_{t_1}^{t_2} \mathrm{FRP}^* \mathrm{d}t \times \beta \times F = \alpha \times \mathrm{FRP} \times f_{\mathrm{FRP}} \times (t_2 - t_1) \times \beta \times F, \quad (1)$$

where E (in g) is the emissions of GHGs; α is a correction factor used to adjust for FRP detection errors between MODIS and VIIRS, which is given a value of 2.5 following Vadrevu and Lasko (2018), indicating that the FRP VIIRS sum is 2.5 times the FRP MODIS sum. t_1 and t_2 are the beginning and ending time of fire spots, respectively. The average burning time (3 h) of a fire spot in Northeast China was obtained by delivering questionnaires to local farmers (Yang et al., 2020). FRP* (in MW) is the adjusted satellite-detected FRP. FRP (in MW) is the instantaneous FRP observed by satellite. f_{FRP} is a correction factor that is used to adjust the underestimated emissions by fire spots, and Yang et al. (2020) determined an optimal value of 5 for f_{FRP} by calibrating the contributions of open straw burning to ground observation data in Northeast China using WRF-CMAQ. β (in $kg\,MJ^{-1}$) is the biomass combustion rate, and the average value of $0.411\,kg\,MJ^{-1}$ from previous studies is used here (Wooster et al., 2005; Freeborn et al., 2008). F (in $g\,kg^{-1}$) is the emission factor for individual straw type (Table 1) (Li et al., 2007; Liu et al., 2011; Peng et al., 2016).

Driving factors such as the output of major grains and rural residential coal consumption for temporal variations of annual GHG emissions were explored through Pearson correlation analysis using SPSS 20.0. Information on the above data is also detailed in Table S1.

3 Results and discussion

3.1 Spatial and temporal distributions of fire spots

Cultivated lands in Northeast China are primarily distributed in Sanjiang Plain (northeastern Heilongjiang Province), Songnen Plain (western Heilongjiang Province and midwestern Jilin Province), and Liao River plain (central Liaoning Province) (Fig. 2a). Fire spots were widely spread, covering most cultivated lands, including both dry and paddy fields across Northeast China (Fig. 2a and b). A total of 156 044 fire spots from open straw burning were recorded during 2001–2020. Note that the traditional method overestimated the total number of fire sports by 7190 over the 20-year period, with the largest in 2017 (an overestimation of 4060) (Fig. 2c). This highlights the importance of integrating crop cycle information into fire spot extraction for open straw burning to enhance data accuracy and reliability. Considering the 20-year period (2001–2020), high occurrence frequencies of open straw burning (also referred to as intensity of fire spots below) appeared in the northern Sanjiang Plain, eastern Songnen Plain, and eastern Liao River plain, as well as scattered areas close to Inner Mongolia (Fig. 2a and b).

Interannual variations of fire spot distributions are shown in Fig. S1. In the Sanjiang Plain, low occurrence frequencies of fire spots were observed in a few cultivated lands during 2003–2006 (Fig. S1c to f) and in most cultivated lands in the northern part of the plain during 2007–2013 (Fig. S1g to m). Note that in 2014 and later years, fire spots were extended to the entire Sanjiang Plain, and the northern part of the plain became an area with a high intensity of fire spots (Fig. S1n to q), although a few cultivated lands in this plain recorded a low intensity of fire spots after 2018 (Fig. S1r to t). In the Songnen Plain, most cultivated lands recorded fire spots from 2014 to 2017, with the highest intensity in the northern and eastern parts of the plain (Fig. S1n to q). The occurrence frequencies of fire spots have decreased across the plain since 2018, particularly in the northern part of the plain (Fig. S1r to t). In the Liao River plain, although fire spots were observed in most cultivated lands in the eastern part of the plain during 2014–2017, high occurrence frequency was only recorded in 2014 (Fig. S1n to q).

Apparently, open straw-burning events have decreased in all of the three plains since 2018 (Fig. S1r to t), which was likely due to the intensified effort from the Chinese government in banning open straw burning (Hong et al., 2023). The reduction in the number of fire spots was more significant in the Sanjiang Plain and northern Songnen Plain than in the Liao River plain (Fig. S1), indicating more compliance with straw-burning bans from state farms in the former two regions.

Fire spots from open straw burning were concentrated in spring and autumn, with few burning events in the other two seasons in Northeast China. Open straw burning events in this region during 2003–2020 can be roughly divided into

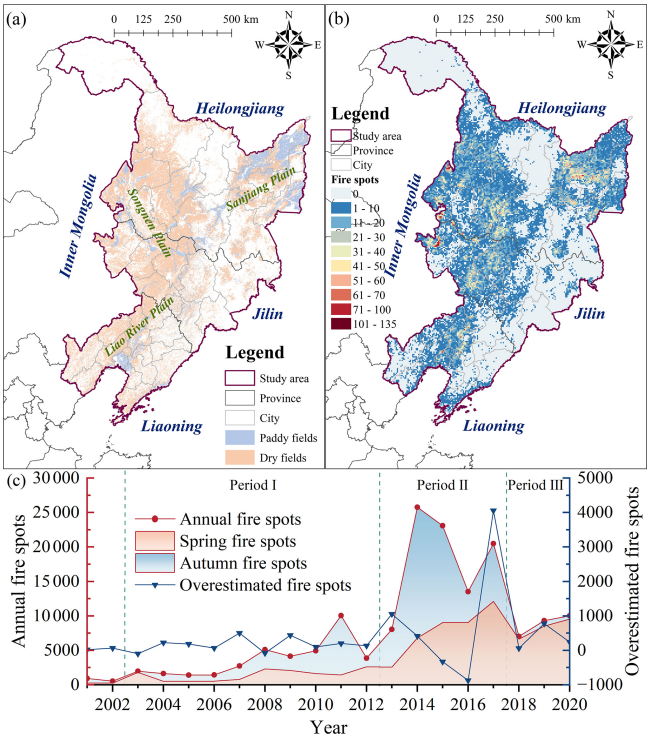

Figure 2. **(a)** Spatial distributions of cultivated land in 2020 in Northeast China (https://www.resdc.cn, last access: 17 November 2023), **(b)** spatial distributions of the total number of fire spots during 2001–2020 in Northeast China, and **(c)** seasonal distributions of the annual fire spots and annual overestimated fire spots with the traditional method from 2001 to 2020. The overestimated fire spots are calculated as the number of fire spots identified by the traditional method minus those extracted by the novel method.

three distinctive periods (Fig. 2c). During Period I (2003–2012), the annual average number of fire spots in this region was 3732. There were more fire spots in autumn than in spring in most of these years. During Period II (2013–2017), there was a substantial surge in fire spots, with an annual average of 18 177 spots, accounting for 58.2 % of the 20-year total. Notably, the number of fire spots peaked at 25 759 in 2014. Spring fire spots consistently increased annually, reaching the highest in 2017 at 12 094 spots. The variations in autumn fire spots fluctuated, with a peak of 18 951 spots in 2014. During 2013–2015, autumn fire spots were higher than spring; however, this trend reversed in 2016 and 2017, with spring fire spots becoming more dominant. During Period III (2018–2020), the number of fire spots experienced a significant decrease, averaging 8788 spots annually, which was a 51.7 % decrease from Period II. Spring emerged as the primary season of fire spots, accounting for approximately 93.8 % of the annual total. Zhao et al. (2021) have reported a similar phenomenon, in which the primary season of open straw burning in Northeast China gradually shifts to spring (April to June). The apparent seasonal variation of

open straw burning primarily stems from strict government bans imposed after the autumn harvest (Yang et al., 2020). In addition, farmers' increasing awareness regarding how open straw burning contributes to the thawing of spring soil may also be a factor (Saxton et al., 1993; Song et al., 2024).

However, the "sudden drop" in fire spots should also be partially attributed to strategies employed by farmers to avoid detection by satellite and government regulations, such as burning straw on smaller scales and in more dispersed areas, or during non-transit times of the satellites (Liu et al., 2019, 2020). Chen et al. (2022) also found that farmers in East China frequently burned straw in 2019 during non-transit times of the MODIS and VIIRS instruments, as indicated by Himawari satellite data. To further verify the reliability of the "sudden drop" in fire spots in Northeast China, we analyzed the trend of particulate matter concentrations (PM_{10} and $PM_{2.5}$) during the periods of open straw burning from 2014 to 2020 in Northeast China (Fig. S2). Atmospheric particulate matter concentrations during autumn open straw burning in Northeast China decreased with a "sudden drop" in fire spots (Fig. S2c). However, a similar trend was not observed in spring (Fig. S2b), possibly due to limitations in fire spot detection by current satellite techniques and avoidance strategies. Kumar et al. (2021) suggested that a hybrid inventory that accurately allocates emissions estimated using the "bottom-up" approach based on satellite data may be more advantageous in this scenario.

The straw-burning dates in Northeast China also changed during the three periods, besides varying with crop type. During Period I (2003–2012), the autumn burning dates of corn and rice straw were concentrated from early October to mid-November (DOY range of 270 to 320). Spring burning dates of corn and rice straw were concentrated between mid-March and late April (DOY range of 70 to 120) in 2003, while the were dispersed from early March to mid-May (DOY range of 60 to 140) in 2012 (Fig. 3a and b). During Period II (2013–2017), the dispersion of spring burning dates for corn and rice straw became more pronounced, extending from early February to mid-May (DOY range of 30 to 140) (Fig. 3a and b). During Period III (2018–2020), the dispersion of spring burning dates for corn and rice straw persisted (Fig. 3a and b). During Period I (2003–2012), the spring and autumn burning dates of bean straw in Heilongjiang Province were concentrated from mid-March to late April (DOY range of 70 to 120) and from early October to mid-November (DOY range of 270 to 320), respectively (Fig. 3c). During 2013–2020, the spring burning dates of bean straw in Northeast China were concentrated between early February and late April (DOY range of 30 to 120), while the autumn burning dates remained consistent with those during Period I in Heilongjiang Province (Fig. 3c). Unlike other crops, the burning dates for wheat straw did not conform to the aforementioned pattern of variation, likely due to a limited number of fire spots (Fig. 3d). The changing dispersion of burning dates for each crop type indicates shifts in agricultural practices

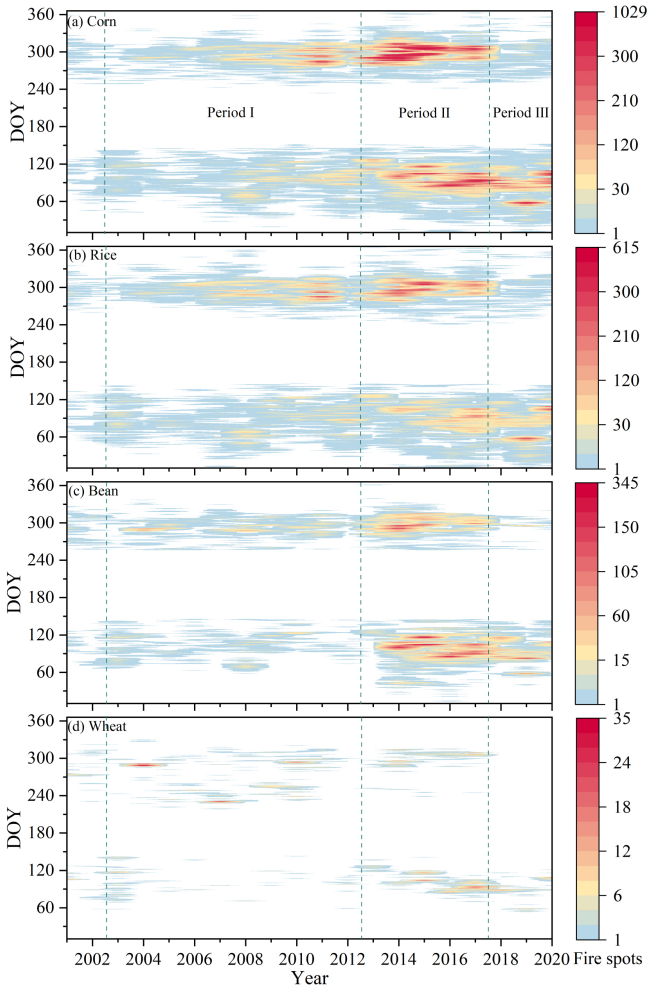

Figure 3. The daily frequency distribution of fire spots from various straw burning: **(a)**, **(b)**, **(c)**, and **(d)** represent corn, rice, bean, and wheat straw, respectively. Note that the *x* axis is year, the *y* axis is DOY, and the range of color bars (indicating fire spots) is different for each crop, with values ranging from 1 to 1029 for corn, 1 to 615 for rice, 1 to 345 for beans, and 1 to 35 for wheat.

that may be influenced by regional straw-burning ban policies, environmental conditions, and farming practices (Yang et al., 2020).

3.2 High-spatial-resolution annual emission inventory of GHGs

The cumulative emissions of CO_2, CH_4, and N_2O from open straw burning in Northeast China from 2001 to 2020 amounted to 198 Tg, 557 Gg, and 15.7 Gg, respectively (or 218 Tg CO_2-eq (equivalent) in total). The spatial distributions of GHG emissions correspond well with those of fire spots, particularly in high-emission areas (Figs. 2 and 4). However, the amounts of GHG emissions in the northern Songnen Plain unexpectedly exceeded those in the eastern Songnen Plain and eastern Liao River plain, suggesting that

even low-intensity fire spots can generate considerable emissions of GHGs due to higher FRP detected via remote sensing. Therefore, the FRP algorithm proves to be more effective than burned-area-based algorithms in identifying emission intensity resulting from open straw burning while reducing the uncertainty associated with high-spatiotemporal-resolution emission inventories (Wu et al., 2023).

The annual emissions of CO_2, CH_4, N_2O, and CO_2-eq from 2001 to 2020 are presented in Figs. S3, S4, S5, and S6, respectively. The spatiotemporal patterns of GHG emissions correspond well to the observed trends in fire spots during Period I (2003–2012). However, during Period II (2013–2017) and Period III (2018–2020), the emissions of GHGs in the eastern Songnen Plain and eastern Liao River plain did not exhibit a proportional increase with the rise in fire spots. This discrepancy can be attributed to the dispersed burning dates among individual farmers in these regions, resulting in high-intensity fire spots with relatively low emissions. In contrast, several state farms located in the northern Sanjiang Plain and northern Songnen Plain demonstrated a higher level of synchronization in open straw-burning activities, resulting in parallel trends between fire spots and emissions (Cui et al., 2021).

During Period I (2003–2012), average annual CO_2-eq emission was at 4.20 Tg, and the cumulative CO_2-eq emission amounted to 42.0 Tg. During Period II (2013–2017), average annual CO_2-eq emission increased substantially to 26.1 Tg, and the cumulative emission during this period amounted to 130 Tg, which accounted for 59.9 % of the total emissions over the 2 decades. During Period III (2018–2020), average annual CO_2-eq emissions decreased significantly to 14.3 Tg, and the cumulative emission during this period amounted to 42.8 Tg (Fig. 5a). The trend of CO_2-eq emission from 2003 to 2020 generally corresponds with the occurrence of fire spots, except for 2015 when higher emissions were obtained despite having fewer fire spots than the case in 2014 (Fig. 5a). Such a trend is consistent with those of carbonaceous gas and aerosol (CGA) emissions estimated by Liu et al. (2022). This discrepancy between fire spots and pollutant emissions in 2015 highlights the limitations of estimating pollutant emissions based solely on burned areas (Ke et al., 2019; Wu et al. 2023). The combustion of corn and rice straw was identified as the primary contributor to CO_2-eq emissions, accounting for 51.1 % and 30.8 %, respectively, of the total emissions (Fig. 5b). Specifically, corn straw burning released 99.6, 9.06, and 2.42 Tg, while rice straw burning released 61.8, 3.78, and 1.27 Tg of CO_2, CO_2-eq for CH_4, and CO_2-eq for N_2O, respectively.

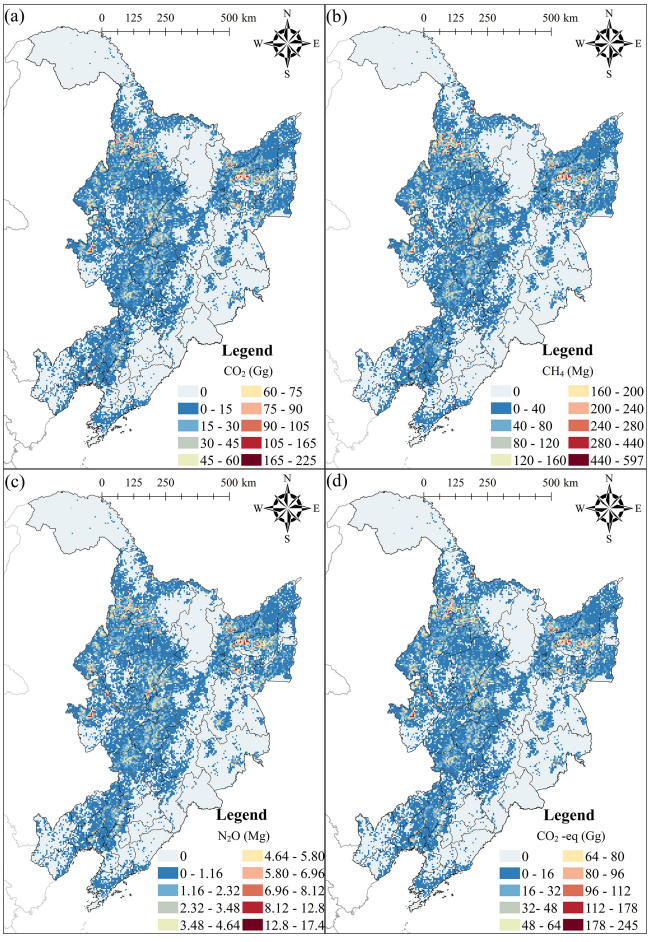

Figure 4. The cumulative GHG emissions from open straw burning in Northeast China from 2001 to 2020 for CO_2 **(a)**, CH_4 **(b)**, N_2O **(c)**, and CO_2-eq **(d)** emissions, respectively. Note that the range of color bars (indicating emissions) is different for each GHG, with values ranging from 0 to 225 Gg for CO_2, 0 to 597 Mg for CH_4, 0 to 17.4 Mg for N_2O, and 0 to 245 Gg for CO_2-eq.

3.3 Validation and limitations

Our estimated total CO_2 emissions from 2012 to 2020 with MODIS (161 Tg) or with VIIRS (165 Tg) were much lower than those (∼ 523 Tg) estimated by Liu et al. (2022); the latter was based on a modified FRP algorithm and fire spot products by VIIRS, which has limitations in its traditional straw extraction methods in accurately identifying fire spots during certain times of the year. Our estimated CO_2 emission from 2002 to 2020 in Northeast China (196 Tg) was slightly lower than that (195 Tg) estimated by Global Fire Emissions Database Version 4.1 (GFED4.1s) by van der Werf et al. (2017) and slightly higher than that (181 Tg) estimated by the Fire INventory from NCAR version 2.5 (FINNv2.5) by Wiedinmyer et al. (2023), which addresses the underestimation of open biomass burning in China by the older version FINNv1.5 (Stavrakou et al., 2016; Yang et al., 2020) (Fig. 6). However, our estimated total CO_2 emission from 2012 to 2020 was significantly higher than that (35.6 Tg) estimated by VIIRS-based Fire Emission Inventory version 0 (VFEIv0) by Ferrada et al. (2022), which relies on the traditional FRP algorithm (Fig. 6). Furthermore, Northeast China surpassed East China (27.1 Tg) as the highest emitter of open straw

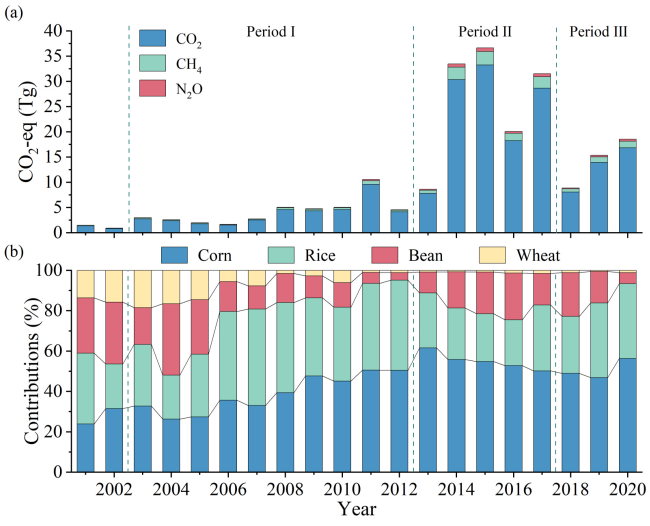

Figure 5. **(a)** Regional total annual CO_2-eq emissions and **(b)** percentage contributions from open burning of individual crop straw type.

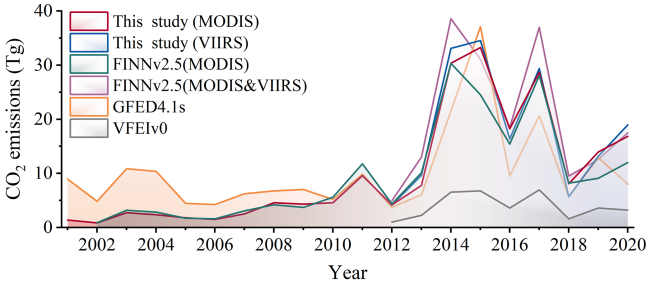

Figure 6. Annual total emissions of CO_2 from open straw burning (agricultural waste burning) in Northeast China from this study with MODIS (red, 2001–2020) and VIIRS (blue, 2012–2020), the Fire INventory from NCAR version 2.5 (FINNv2.5) with MODIS-only (green, 2002–2020), FINNv2.5 with MODIS and VIIRS (purple, 2012–2020), Global Fire Emissions Database Version 4.1 (GFED4.1s) (orange, 2001–2020), and VIIRS-based Fire Emission Inventory version 0 (VFEIv0) (grey, 2012–2020).

burning in China since 2014, with CO_2 emissions reaching 30.4 Tg (Zhang et al., 2020).

Although this study effectively improved the accuracy of emission inventory for open straw burning through the novel method that integrates crop cycle information into extraction and classification of fire spots and the modified FRP algorithm, certain limitations still exist. The uncertainty in this study stems mainly from the inherent limitations of satellite fire detection systems. The MODIS fire spot product, although widely used, is limited by its temporal resolution and tends to miss transient or small-scale fires. In addition, straw burning during non-satellite transit periods, on cloudy days, at night, and under heavy haze further exacerbates the underestimation of fire incidence, leading to potential gaps in emission inventories.

Additionally, the novel method that integrates crop cycle information into extraction and classification of fire spots presents a promising advancement. However, its applicability is constrained to regions where comprehensive and detailed crop data are available. In countries or regions lacking such agricultural information, this method may face challenges, thereby limiting its broader applicability. These factors underscore the need for continued refinement of satellite detection technologies and the expansion of agricultural data collection efforts to reduce uncertainties and enhance the robustness of emission inventories on regional to global scales.

3.4 Driving factors of open straw burning

Open straw burning is more prominently influenced by anthropogenic activities compared to other types of open biomass burning, such as forest, shrubland, and grassland fires (Syphard et al., 2017; Wu et al., 2020). Open straw burning is influenced by changes in straw yield and utilization rate, straw-burning ban policy, and farmers' awareness of straw-burning consequences (Chen et al., 2016; Li et al., 2017; Tao et al., 2018; Fang et al., 2019; Xu and You, 2023).

Northeast China has experienced a remarkable expansion in its sown area for major grain crops over the past 2 decades. By 2020, the sown area reached 231 937 km^2, 61.4 % more than that in 2001 (National Bureau of Statistics of China, 2002–2021). In the meantime, annual straw yield reached 143 Tg in 2020, 142 % higher than that (59.2 Tg) in 2001 (Fig. 7) (numbers are calculated based on the major grain yields in Northeast China presented in the National Bureau of Statistics of China (2002–2021) and the ratio of straw and grain (Wang et al., 2012)). Note that the annual straw yields have stabilized around 140 Tg since 2017, and this trend is expected to persist for many years to come (Fig. 7). From 2003 to 2020, a strong positive correlation was observed between the straw yields and the emissions of CO_2-eq from open straw burning across Northeast China, as well as in Heilongjiang and Jilin provinces ($p < 0.01$, Table S2). When looking at individual periods, significant correlations were only observed during Period I (2003–2012) for the whole of Northeast China ($p < 0.01$) and Heilongjiang ($p < 0.01$) (Table S2). This highlights that increased straw yields exacerbated the challenges of straw disposal in Northeast China and have been a major contributor to the increase in the emissions of GHGs from open straw burning in the aforementioned region and period.

Besides open burning, crop straw is also used for cooking and heating in rural households in Northeast China (Ke et al., 2023; Liu et al., 2023). Crop straw can also be converted to bioenergy, used as animal feed, and returned to the fields (Alengebawy et al., 2022; Fang et al., 2022). However, exact quantification of straw utilization in different sectors in Northeast China is still lacking (Shi et al., 2023). Knowing that coal combustion and straw burning are major energy sources for rural households in Northeast China, we

tried to explore potential changes in straw utilization on open straw burning through coal consumption changes (Fang et al., 2019). The abrupt increase in rural residential coal consumption in 2013 in Northeast China coincided with a spike in CO_2-eq emissions from open straw burning (Fig. 7a). Furthermore, a significant positive correlation between rural residential coal consumption and CO_2-eq emissions in Northeast China was revealed, especially in Heilongjiang and Jilin provinces (Table S3). We thus speculate that the increase in rural commercial energy consumption may have reduced the demand for straw as an energy source for agricultural households, thus facilitating the increased open straw burning. This needs to be confirmed in future studies once various straw utilization pathways are quantified.

We also evaluated the efficacy of straw-burning ban policy in Heilongjiang, Jilin, and Liaoning (Table S4). Despite the implementation of the policy in 2013 in this region, a significant reduction in CO_2-eq emissions from open straw burning was only observed after 2018 (Fig. 7). Compared to the other regions of China, the effective control of open straw burning was delayed by several years in Northeast China (Huang et al., 2021). An important phenomenon was observed regarding the geographical and temporal expansion of the ban policy, for example, initially focused on key areas and specific seasons (autumn and winter) and progressively extended to the entire region and throughout the whole year (see Heilongjiang Province as an example; Table S4). Therefore, enhanced enforcement of the ban policy likely reduced CO_2-eq emissions during Period III and shifted the burning season to spring.

In conclusion, the enforcement of region-specific straw-burning bans tailored to spatiotemporal variations is crucial to control GHG emissions, given the anticipated sustained high straw yields in the future. Additionally, promoting diverse methods for utilizing straw is highlighted as an effective strategy for mitigating carbon emissions resulting from open straw burning in Northeast China. A combined effort of policy enforcement and alternative straw usage would play a pivotal role in addressing the environmental challenges posed by agricultural practices in the region.

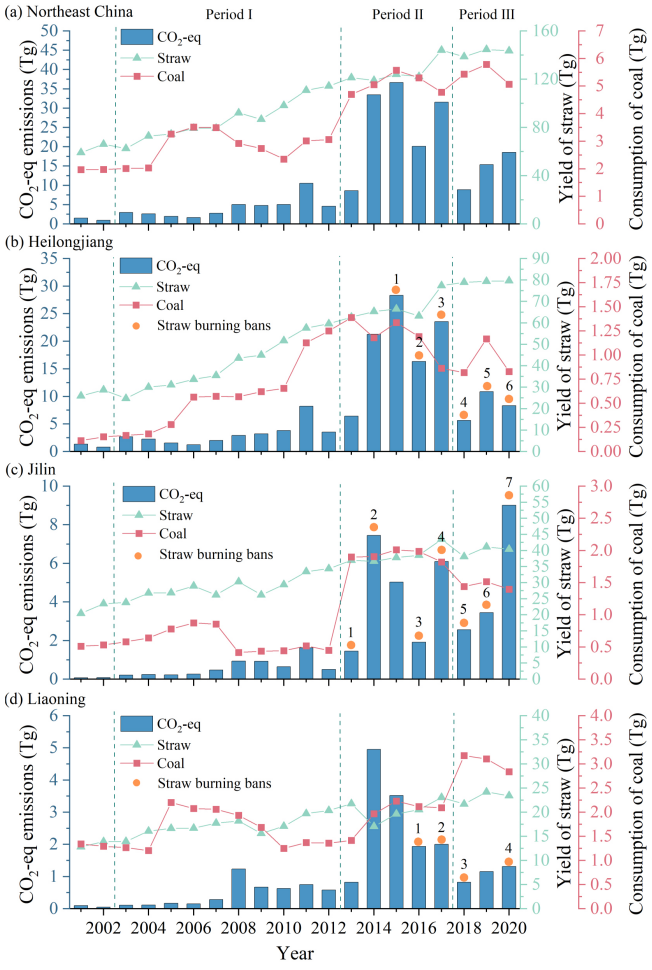

Figure 7. Annual CO_2-eq emissions, yield of straw, rural residential coal consumption, and straw-burning bans in **(a)** Northeast China, **(b)** Heilongjiang, **(c)** Jilin, and **(d)** Liaoning from 2001 to 2020. Note that the range of the *y* axis is different for each region. The blue *y* axis indicates CO_2-eq emissions, with values ranging from 0 to 50 Tg for Northeast China, 0 to 35 Tg for Heilongjiang, 0 to 10 Tg for Jilin, and 0 to 6 Tg for Liaoning. The green *y* axis indicates yield of straw, with values ranging from 0 to 160 Tg for Northeast China, 0 to 90 Tg for Heilongjiang, 0 to 60 Tg for Jilin, and 0 to 40 Tg for Liaoning. The red *y* axis indicates rural residential coal consumption, with values ranging from 0 to 7 Tg for Northeast China, 0 to 2 Tg for Heilongjiang, 0 to 3 Tg for Jilin, and 0 to 4 Tg for Liaoning.

4 Conclusions

This study provides a comprehensive analysis of the spatiotemporal variations of open straw burning across Northeast China from 2001 to 2020 and develops regional-scale high-spatial-resolution annual emission inventories of GHGs. Open straw burning in Northeast China emitted a total of 218 Tg of CO_2-eq during 2001–2020, of which 19.3 % was from Period I (2003–2012), 59.9 % from Period II (2013–2017), and 19.7 % from Period III (2018–2020). Analysis results demonstrate the necessity of integrating the crop cycle information into the extraction and classification of fire spots from open straw burning to enhance the accuracy of emission inventories of various pollutants. This study also highlights the inconsistencies between the number of fire spots and pollutant emissions caused by remote sensing detection techniques. In Northeast China, regions such as the northern Sanjiang Plain, eastern and northern Songnen Plain, and eastern Liao River plain are identified as high-emission areas of GHGs from open straw burning, which emitted 38.1, 45.5, 31.9, and 10.8 Tg of CO_2-eq, respectively, during 2001–2020. Additionally, it is observed that the season for open straw burning has shifted from au-

tumn to spring, with dispersed burning dates. This spatiotemporal analysis provides crucial insights into policy effectiveness as well as geographical variations regarding compliance with regulations banning open straw burning. Consequently, government policies prohibiting open straw burning should be adjusted according to the observed spatiotemporal variations in different regions. Simultaneously promoting diversified applications of straw, such as bioenergy conversion, animal feeding, and soil amendment, is recommended – a strategy that is aligned with China's dual-carbon objectives aiming at achieving carbon peak and carbon neutrality.

Data availability. All data are archived and are available upon request (cuisong-bq@neau.edu.cn and songzihan@neau.edu.cn).

Supplement. The supplement related to this article is available online at: https://doi.org/10.5194/acp-24-13101-2024-supplement.

Author contributions. SC, QF, and DL contributed to the research design; ZHS and RZ contributed to the investigation; ZHS, LZ, CT, QF, and ZXS designed the methodology; ZHS completed data curation; ZHS, LZ, CT, and SC completed the writing and visualization of the manuscript; SC supervised and acquired funds.

Competing interests. At least one of the (co-)authors is a member of the editorial board of *Atmospheric Chemistry and Physics*. The peer-review process was guided by an independent editor, and the authors also have no other competing interests to declare.

Disclaimer. Publisher's note: Copernicus Publications remains neutral with regard to jurisdictional claims made in the text, published maps, institutional affiliations, or any other geographical representation in this paper. While Copernicus Publications makes every effort to include appropriate place names, the final responsibility lies with the authors.

Acknowledgements. We acknowledge the MCD14ML dataset provided by the University of Maryland, the ChinaCropArea1 km and ChinaCropPhen1 km datasets provided by the State Key Laboratory of Earth Surface Processes and Resource Ecology & Ministry of Education Key Laboratory of Environmental Change and Natural Hazards at Beijing Normal University, the Heilongjiang soybean map provided by the Ministry of Education Key Laboratory for Earth System Modeling at Tsinghua University, and the crop classification maps for Northeast China provided by the China Agricultural University.

Financial support. This research has been supported by the Distinguished Youth Science Foundation of Heilongjiang Province (grant no. JQ2023E001) and Young Leading Talents of Northeast Agricultural University (grant nos. NEAU2023QNLJ-013 and NEAU2024QNLJ-01).

Review statement. This paper was edited by Tanja Schuck and reviewed by two anonymous referees.

References

Ahmed, W., Tan, Q., Ali, S., and Ahmad, N.: Addressing environmental implications of crop stubble burning in Pakistan: innovation platforms as an alternative approach, Int. J. Global Warming, 19, 76–93, https://doi.org/10.1504/IJGW.2019.101773, 2019.

Alengebawy, A., Mohamed, B. A., Ran, Y., Yang, Y., Pezzuolo, A., Samer, M., and Ai, P.: A comparative environmental life cycle assessment of rice straw-based bioenergy projects in China, Environ. Res., 212, 113404, https://doi.org/10.1016/j.envres.2022.113404, 2022.

Chen, J. X., Li, R., Tao, M. H., Wang, L. L., Lin, C. Q., Wang, J., Wang, L. C., Wang, Y., and Chen, L .F.: Overview of the performance of satellite fire products in China: Uncertainties and challenges, Atmos. Environ., 268, 118838, https://doi.org/10.1016/j.atmosenv.2021.118838, 2022.

Chen, Y. L., Shen, H. Z., Zhong, Q. R., Chen, H., Huang, T. B., Liu, J. F., Cheng, H. F., Zeng, E. Y., Smith, K. R., and Tao, S.: Transition of household cookfuels in China from 2010 to 2012, Appl. Energ., 184, 800–809, https://doi.org/10.1016/j.apenergy.2016.07.136, 2016.

Cui, S., Song, Z. H., Zhang, L. M., Shen, Z. X., Hough, R., Zhang, Z. L., An, L. H., Fu, Q., Zhao, Y. C., and Jia, Z. Y.: Spatial and temporal variations of open straw burning based on fire spots in northeast China from 2013 to 2017, Atmos. Environ., 244, 117962, https://doi.org/10.1016/j.atmosenv.2020.117962, 2021.

Fang, Y. R., Wu, Y., and Xie, G. H.: Crop residue utilizations and potential for bioethanol production in China, Renew. Sust. Energ. Rev., 113, 109288, https://doi.org/10.1016/j.rser.2019.109288, 2019.

Fang, Y. R., Zhang, S. L., Zhou, Z. Q., Shi, W. J., and Xie, G. H.: Sustainable development in China: Valuation of bioenergy potential and CO_2 reduction from crop straw, Appl. Energ., 322, 119439, https://doi.org/10.1016/j.apenergy.2022.119439, 2022.

Ferrada, G. A., Zhou, M., Wang, J., Lyapustin, A., Wang, Y. J., Freitas, S. R., and Carmichael, G. R.: Introducing the VIIRS-based Fire Emission Inventory version 0 (VFEIv0), Geosci. Model Dev., 15, 8085–8109, https://doi.org/10.5194/gmd-15-8085-2022, 2022.

Freeborn, P. H., Wooster, M. J., Hao, W. M., Ryan, C. A., Nordgren, B. L., Baker, S. P., and Ichoku, C.: Relationships between energy release, fuel mass loss, and trace gas and aerosol emissions during laboratory biomass fires, J. Geophys. Res.-Atmos., 113, D01301, https://doi.org/10.1029/2007JD008679, 2008.

Fu, J., Song, S. T., Guo, L., Chen, W. W., Wang, P., Duanmu, L. J., Shang, Y. J., Shi, B. W., and He, L. Y.: Interprovincial joint prevention and control of open straw burning in Northeast China: Implications for atmospheric environment management, Remote Sens., 14, 2528, https://doi.org/10.3390/rs14112528, 2022.

Gadde, B., Bonnet, S., Menke, C., and Garivait, S.: Air pollutant emissions from rice straw open field burning in India,

Thailand and the Philippines, Environ. Pollut., 157, 1554–1558, https://doi.org/10.1016/j.envpol.2009.01.004, 2009.

Giglio, L., Schroeder, W., and Justice, C. O.: The collection 6 MODIS active fire detection algorithm and fire products, Remote Sens. Environ., 178, 31–41, https://doi.org/10.1016/j.rse.2016.02.054, 2016.

Guan, Y. N., Chen, G. Y., Cheng, Z. J., Yan, B. B., and Hou, L. A.: Air pollutant emissions from straw open burning: A case study in Tianjin, Atmos. Environ., 171, 155–164, https://doi.org/10.1016/j.atmosenv.2017.10.020, 2017.

Hong, X. H., Zhang, C. X., Tian, Y., Wu, H. Y., Zhu, Y. Z., and Liu, C.: Quantification and evaluation of atmospheric emissions from crop residue burning constrained by satellite observations in China during 2016–2020, Sci. Total. Environ., 865, 161237, https://doi.org/10.1016/j.scitotenv.2022.161237, 2023.

Huang, K., Zhuang, G., Lin, Y., Wang, Q., Fu, J. S., Fu, Q., Liu, T., and Deng, C.: How to improve the air quality over megacities in China: pollution characterization and source analysis in Shanghai before, during, and after the 2010 World Expo, Atmos. Chem. Phys., 13, 5927–5942, https://doi.org/10.5194/acp-13-5927-2013, 2013.

Huang, L., Zhu, Y. H., Liu, H. Q., Wang, Y. J., Allen, D. T., Ooi, M. C. G., Manomaiphiboon, K., Latif, M. T., Chan, A., and Li, L.: Assessing the contribution of open crop straw burning to ground-level ozone and associated health impacts in China and the effectiveness of straw burning bans, Environ. Int., 171, 107710, https://doi.org/10.1016/j.envint.2022.107710, 2023.

Huang, L., Zhu, Y. H., Wang, Q., Zhu, A. S., Liu, Z. Y., Wang, Y. J., Allen, D. T., and Li, L.: Assessment of the effects of straw burning bans in China: Emissions, air quality, and health impacts, Sci. Total Environ., 789, 147935, https://doi.org/10.1016/j.scitotenv.2021.147935, 2021.

Huang, X., Li, M. M., Li, J. F., and Song, Y.: A high-resolution emission inventory of crop burning in fields in China based on MODIS Thermal Anomalies/Fire products, Atmos. Environ., 50, 9–15, https://doi.org/10.1016/j.atmosenv.2012.01.017, 2012.

Jin, Q. F., Ma, X. Q., Wang, W. H., Yang, S. Y., and Guo, F. T.: Temporal and spatial variations of $PM_{2.5}$ emissions from crop straw burning in eastern China during 2000–2014, Acta Sci. Circumstantiae, 37, 460–468, 2017 (in Chinese).

Jin, Q. F., Ma, X. Q., Wang, G. Y., Yang, X. J., and Guo, F. T.: Dynamics of major air pollutants from crop residue burning in mainland China, 2000–2014, J. Environ. Sci., 70, 190–205, https://doi.org/10.1016/j.jes.2017.11.024, 2018.

Ke, H. B., Gong, S. L., He, J. J., Zhou, C. H., Zhang, L., and Zhou, Y. K.: Spatial and temporal distribution of open bio-mass burning in China from 2013 to 2017, Atmos. Environ., 210, 156–165, https://doi.org/10.1016/j.atmosenv.2019.04.039, 2019.

Ke, Y. X., Zhang, F. X., Zhang, Z. L., Hough, R., Fu, Q., Li, Y. F., and Cui, S.: Effect of combined aging treatment on biochar adsorption and speciation distribution for Cd (II), Sci. Total Environ., 867, 161593, https://doi.org/10.1016/j.scitotenv.2023.161593, 2023.

Korontzi, S., McCarty, J., Loboda, T., Kumar, S., and Justice, C.: Global distribution of agricultural fires in croplands from 3 years of Moderate Resolution Imaging Spectroradiometer (MODIS) data, Global Biogeochem. Cy., 20, GB2021, https://doi.org/10.1029/2005GB002529, 2006.

Kumar, A., Hakkim, H., Sinha, B., and Sinha, V.: Gridded 1 km × 1 km emission inventory for paddy stubble burning emissions over north-west India constrained by measured emission factors of 77 VOCs and district-wise crop yield data, Sci. Total Environ., 789, 48064, https://doi.org/10.1016/j.scitotenv.2021.148064, 2021.

Li, C., Hu, Y., Zhang, F., Chen, J., Ma, Z., Ye, X., Yang, X., Wang, L., Tang, X., Zhang, R., Mu, M., Wang, G., Kan, H., Wang, X., and Mellouki, A.: Multi-pollutant emissions from the burning of major agricultural residues in China and the related health-economic effects, Atmos. Chem. Phys., 17, 4957–4988, https://doi.org/10.5194/acp-17-4957-2017, 2017.

Li, X. H., Wang, S. X., Duan, L., Hao, J. M., Li, C., Chen, Y. S., and Yang, L.: Particulate and trace gas emissions from open burning of wheat straw and corn stover in China, Environ. Sci. Technol., 41, 6052–6058, https://doi.org/10.1021/es0705137, 2007.

Li, X. Y., Yu, L., Peng, D. L., and Gong, P.: A large-scale, long time-series (1984–2020) of soybean mapping with phenological features: Heilongjiang Province as a test case, Int. J. Remote Sens., 42, 7332–7356, https://doi.org/10.1080/01431161.2021.1957177, 2021.

Liu, L. H., Jiang, J. Y., and Zong, L. G.: Emission inventory of greenhouse gases from agricultural residues combustion: A case study of Jiangsu Province, Environ. Sci., 32, 1242–1248, 2011 (in Chinese).

Liu, T. J., Marlier, M. E., Karambelas, A., Jain, M., Singh, S., Singh, M. K., Gautam, R., and DeFries, R. S.: Missing emissions from post-monsoon agricultural fires in northwestern India: regional limitations of MODIS burned area and active fire products, Environ. Res. Commun., 1, 011007, https://doi.org/10.1088/2515-7620/ab056c, 2019.

Liu, T. J., Mickley, L. J., Singh, S., Jain, M., DeFries, R. S., and Marlier, M. E.: Crop residue burning practices across north India inferred from household survey data: Bridging gaps in satellite observations, Atmos. Environ.-X, 8, 100091, https://doi.org/10.1016/j.aeaoa.2020.100091, 2020.

Liu, Y. X., Zhao, H. M., Zhao, G. Y., Zhang, X. L., and Xiu, A. J.: Carbonaceous gas and aerosol emissions from biomass burning in China from 2012 to 2021, J. Clean. Prod., 362, 132199, https://doi.org/10.1016/j.jclepro.2022.132199, 2022.

Liu, Y. Z., Zhang, J., and Zhuang, M. H.: Bottom-up re-estimations of greenhouse gas and atmospheric pollutants derived from straw burning of three cereal crops production in China based on a national questionnaire, Environ. Sci. Pollut. Res., 28, 65410–65415, https://doi.org/10.1007/s11356-021-15658-9, 2021.

Liu, Z. K., Cui, S., Fu, Q., Zhang, F. X., Zhang, Z. L., Hough, R., An, L. H., Li, Y. F., and Zhang, L. M.: Transport of neonicotinoid insecticides in a wetland ecosystem: has the cultivation of different crops become the major sources?, J. Environ. Manag., 339, 117838, https://doi.org/10.1016/j.scitotenv.2023.161593, 2023.

Luo, Y. C., Zhang, Z., Li, Z. Y., Chen, Y., Zhang, L. L., Cao, J., and Tao, F. L.: Identifying the spatiotemporal changes of annual harvesting areas for three staple crops in China by integrating multi-data sources, Environ. Res. Lett., 15, 074003, https://doi.org/10.1088/1748-9326/ab80f0, 2020a.

Luo, Y., Zhang, Z., Chen, Y., Li, Z., and Tao, F.: ChinaCropPhen1km: a high-resolution crop phenological dataset for three staple crops in China during 2000–2015 based on leaf area

index (LAI) products, Earth Syst. Sci. Data, 12, 197–214, https://doi.org/10.5194/essd-12-197-2020, 2020b.

Lv, Q. C., Yang, Z. Y., Chen, Z. Y., Li, M. C., Gao, B. B., Yang, J., Chen, X., and Xu, B.: Crop residue burning in China (2019–2021): Spatiotemporal patterns, environmental impact, and emission dynamics, Environ. Sci. Ecotechnol., 21, 100394, https://doi.org/10.1016/j.ese.2024.100394, 2024.

Mehmood, K., Wu, Y., Wang, L., Yu, S., Li, P., Chen, X., Li, Z., Zhang, Y., Li, M., Liu, W., Wang, Y., Liu, Z., Zhu, Y., Rosenfeld, D., and Seinfeld, J. H.: Relative effects of open biomass burning and open crop straw burning on haze formation over central and eastern China: modeling study driven by constrained emissions, Atmos. Chem. Phys., 20, 2419–2443, https://doi.org/10.5194/acp-20-2419-2020, 2020.

National Bureau of Statistics of China (NBSC): China Statistical Yearbook, China Statistics Press, Beijing, http://www.stats.gov.cn/sj/ndsj/ (last access: 17 November 2023), 2002–2021 (in Chinese).

Pan, X., Kanaya, Y., Taketani, F., Miyakawa, T., Inomata, S., Komazaki, Y., Tanimoto, H., Wang, Z., Uno, I., and Wang, Z.: Emission characteristics of refractory black carbon aerosols from fresh biomass burning: a perspective from laboratory experiments, Atmos. Chem. Phys., 17, 13001–13016, https://doi.org/10.5194/acp-17-13001-2017, 2017.

Peng, L. Q., Zhang, Q., and He, K. B.: Emissions inventory of atmospheric pollutants from open burning of crop residues in China based on a national questionnaire, Res. Environ. Sci., 29, 1109–1118, 2016 (in Chinese).

Saxton, K. E., Kenny, J. F., and McCool, D. K.: Air permeability to define frozen soil infiltration with variable tillage and residue, Trans. ASABE, 36, 1369–1375, https://doi.org/10.13031/2013.28472, 1993.

Schroeder, W., Oliva, P., Giglio, L., and Csiszar, I. A.: The New VIIRS 375 m active fire detection data product: Algorithm description and initial assessment, Remote Sens. Environ., 143, 85–96, https://doi.org/10.1016/j.rse.2013.12.008, 2014.

Shi, W. J., Fang, Y. R., Chang, Y. Y., and Xie, G. H.: Toward sustainable utilization of crop straw: Greenhouse gas emissions and their reduction potential from 1950 to 2021 in China, Resour. Conserv. Recy., 190, 106824, https://doi.org/10.1016/j.resconrec.2022.106824, 2023.

Song, Z. H., Zhang, L. M., Tian, C. G., Li, K. Y., Chen, P. Y., Jia, Z. Y., Hu, P., and Cui, S.: Chemical characteristics, distribution patterns, and source apportionment of particulate elements and inorganic ions in snowpack in Harbin, China, Chemosphere, 349, 140886, https://doi.org/10.1016/j.chemosphere.2023.140886, 2024.

Stavrakou, T., Müller, J. F., Bauwens, M., De Smedt, I., Lerot, C., Van Roozendael, M., Coheur, P. F., Clerbaux, C., Boersma, K. F., van der A, R., and Song, Y.: Substantial underestimation of post-harvest burning emissions in the North China plain revealed by multi-species space observations, Sci. Rep., 6, 32307, https://doi.org/10.1038/srep32307, 2016.

Stockwell, C. E., Yokelson, R. J., Kreidenweis, S. M., Robinson, A. L., DeMott, P. J., Sullivan, R. C., Reardon, J., Ryan, K. C., Griffith, D. W. T., and Stevens, L.: Trace gas emissions from combustion of peat, crop residue, domestic biofuels, grasses, and other fuels: configuration and Fourier transform infrared (FTIR) component of the fourth Fire Lab at Missoula Experiment (FLAME-4), Atmos. Chem. Phys., 14, 9727–9754, https://doi.org/10.5194/acp-14-9727-2014, 2014.

Sun, J. F., Peng, H. Y., Chen, J. M., Wang, X. M., Wei, M., Li, W. J., Yang, L. X., Zhang, Q. Z., Wang, W. X., and Mellouki, A.: An estimation of CO_2 emission via agricultural crop residue open field burning in China from 1996 to 2013, J. Clean. Prod., 112, 2625–2631, https://doi.org/10.1016/j.jclepro.2015.09.112, 2016.

Syphard, A. D., Keeley, J. E., Pfaff, A. H., and Ferschweiler, K.: Human presence diminishes the importance of climate in driving fire activity across the United States, P. Natl. Acad. Sci. USA, 114, 13750–13755, https://doi.org/10.1073/pnas.1713885114, 2017.

Tang, R., Huang, X., Zhou, D., and Ding, A.: Biomass-burning-induced surface darkening and its impact on regional meteorology in eastern China, Atmos. Chem. Phys., 20, 6177–6191, https://doi.org/10.5194/acp-20-6177-2020, 2020.

Tao, S., Ru, M. Y., Du, W., Zhu, X., Zhong, Q. R., Li, B. G., Shen, G. F., Pan, X. L., Meng, W. J., Chen, Y. L., Shen, H. Z., Lin, N., Su, S., Zhuo, S. J., Huang, T. B., Xu, Y., Yun, X., Liu, J. F., Wang, X. L., Liu, W. X., Cheng, H. F., and Zhu, D. Q.: Quantifying the rural residential energy transition in China from 1992 to 2012 through a representative national survey, Nat. Energy, 3, 567–573, https://doi.org/10.1038/s41560-018-0158-4, 2018.

Tian, H. Z., Zhao, D., and Wang, Y.: Emission inventories of atmospheric pollutants discharged from biomass burning in China, Acta Sci. Circumstantiae, 31, 349–357, 2011 (in Chinese).

Vadrevu, K. and Lasko, K.: Intercomparison of MODIS AQUA and VIIRS I-Band fires and emissions in an agricultural landscape-implications for air pollution research, Remote Sens., 10, 978, https://doi.org/10.3390/rs10070978, 2018.

van der Werf, G. R., Randerson, J. T., Giglio, L., van Leeuwen, T. T., Chen, Y., Rogers, B. M., Mu, M. Q., van Marle, M. J. E., Morton, D. C., Collatz, G. J., Yokelson, R. J., and Kasibhatla, P. S.: Global fire emissions estimates during 1997–2016, Earth Syst. Sci. Data, 9, 697–720, https://doi.org/10.5194/essd-9-697-2017, 2017.

Vermote, E., Ellicott, E., Dubovik, O., Lapyonok, T., Chin, M., Giglio, L., and Roberts, G. J.: An approach to estimate global biomass burning emissions of organic and black carbon from MODIS fire radiative power, J. Geophys. Res., 114, D18, https://doi.org/10.1029/2008jd011188, 2009.

Wang, J. Y., Xi, F. M., Liu, Z., Bing, L. F., Alsaedi, A., Hayat, T., Ahmad, B., and Guan, D. D.: The spatiotemporal features of greenhouse gases emissions from biomass burning in China from 2000 to 2012, J. Clean. Prod., 181, 801–808, https://doi.org/10.1016/j.jclepro.2018.01.206, 2018.

Wang, X. Y., Xue, S., and Xie, G. H.: Value-taking for residue factor as a parameter to assess the field residue of field crops, J. China Agr. Univ., 17.1, 1–8, 2012 (in Chinese).

Weldemichael, Y. and Assefa, G.: Assessing the energy production and GHG (greenhouse gas) emissions mitigation potential of biomass resources for Alberta, J. Clean. Prod., 112, 4257–4264, https://doi.org/10.1016/j.jclepro.2015.08.118, 2016.

Wen, X., Chen, W. W., Chen, B., Yang, C. J., Tu, G., and Cheng, T. H.: Does the prohibition on open burning of straw mitigate air pollution? An empirical study in Jilin Province of China in the post-harvest season, J. Environ. Manage., 264, 110451, https://doi.org/10.1016/j.jenvman.2020.110451, 2020.

Wiedinmyer, C., Kimura, Y., McDonald-Buller, E. C., Emmons, L. K., Buchholz, R. R., Tang, W., Seto, K., Joseph, M. B., Barsanti,

K. C., Carlton, A. G., and Yokelson, R.: The Fire Inventory from NCAR version 2.5: an updated global fire emissions model for climate and chemistry applications, Geosci. Model Dev., 16, 3873–3891, https://doi.org/10.5194/gmd-16-3873-2023, 2023.

Wiedinmyer, C., Yokelson, R. J., and Gullett, B. K.: Global emissions of trace gases, particulate matter, and hazardous air pollutants from open burning of domestic waste, Environ. Sci. Technol., 48, 16, 9523–9530, https://doi.org/10.1021/es502250z, 2014.

Wooster, M. J., Roberts, G., Perry, G. L. W., and Kaufman, Y. J.: Retrieval of biomass combustion rates and totals from fire radiative power observations: FRP derivation and calibration relationships between biomass consumption and fire radiative energy release, J. Geophys. Res.-Atmos., 110, D24311, https://doi.org/10.1029/2005JD006318, 2005.

Wu, B. B., Li, J. H., Yao, Z. L., Li, X., Wang, W. J., Wu, Z. C., and Zhou, Q.: Characteristics and reduction assessment of GHG emissions from crop residue open burning in China under the targets of carbon peak and carbon neutrality, Sci. Total Environ., 905, 167235, https://doi.org/10.1016/j.scitotenv.2023.167235, 2023.

Wu, J., Kong, S., Wu, F., Cheng, Y., Zheng, S., Yan, Q., Zheng, H., Yang, G., Zheng, M., Liu, D., Zhao, D., and Qi, S.: Estimating the open biomass burning emissions in central and eastern China from 2003 to 2015 based on satellite observation, Atmos. Chem. Phys., 18, 11623–11646, https://doi.org/10.5194/acp-18-11623-2018, 2018.

Wu, J., Kong, S. F., Wu, F. Q., Cheng, Y., Zheng, S. R., Qin, S., Liu, X., Yan, Q., Zheng, H., Zheng, M. M., Yan, Y. Y., Liu, D. T., Ding, S., Zhao, D. L., Shen, G. F., Zhao, T. L., and Qi, S. H.: The moving of high emission for biomass burning in China: View from multi-year emission estimation and human-driven forces, Environ. Int., 142, 105812, https://doi.org/10.1016/j.envint.2020.105812, 2020.

Xu, C. and You, C.: Agricultural expansion dominates rapid increases in cropland fires in Asia, Environ. Int., 179, 108189, https://doi.org/10.1016/j.envint.2023.108189, 2023.

Xu, R. B., Ye, T. T., Yue, X., Yang, Z. Y., Yu, W. H., Zhang, Y. W., Bell, M. L., Morawska, L., Yu, P., Zhang, Y. X., Wu, Y., Liu, Y. M., Johnston, F., Lei, Y. D., Abramson, M. J., Guo, Y. M., and Li, S. S.: Global population exposure to landscape fire air pollution from 2000 to 2019, Nature, 621, 521–529, https://doi.org/10.1038/s41586-023-06398-6, 2023.

Xu, W. D., Wooster, M. J., Kaneko, T., He, J. P., Zhang, T. R., and Fisher, D.: Major advances in geostationary fire radiative power (FRP) retrieval over Asia and Australia stemming from use of Himarawi-8 AHI, Remote Sens. Environ., 193, 138–149, https://doi.org/10.1016/j.rse.2017.02.024, 2017.

Xuan, F., Dong, Y., Li, J. Y., Li, X. C., Su, W., Huang, X. D., Huang, J. X., Xie, Z. X., Li, Z. Q., Liu, H., Tao, W. C., Wen, Y. A., and Zhang, Y.: Mapping crop type in Northeast China during 2013-2021 using automatic sampling and tile-based image classification, Int. J. Appl. Earth Obs., 117, 103178, https://doi.org/10.1016/j.jag.2022.103178, 2023.

Yang, G. Y., Zhao, H. M., Tong, D. Q., Xiu, A. J., Zhang, X. L., and Gao, C.: Impacts of post-harvest open biomass burning and burning ban policy on severe haze in the Northeastern China, Sci. Total Environ., 716, 136517, https://doi.org/10.1016/j.scitotenv.2020.136517, 2020.

Yang, Y. and Zhao, Y.: Quantification and evaluation of atmospheric pollutant emissions from open biomass burning with multiple methods: a case study for the Yangtze River Delta region, China, Atmos. Chem. Phys., 19, 327–348, https://doi.org/10.5194/acp-19-327-2019, 2019.

Ying, L. X., Shen, Z. H., Yang, M. Z., and Piao, S. L.: Wildfire detection probability of modis fire products under the constraint of environmental factors: A study based on confirmed ground wildfire records, Remote Sens., 11, 3031, https://doi.org/10.3390/rs11243031, 2019.

Zhang, X. H., Lu, Y., Wang, Q. G., and Qian, X.: A high-resolution inventory of air pollutant emissions from crop residue burning in China, Atmos. Environ., 213, 207–214, https://doi.org/10.1016/j.atmosenv.2019.06.009, 2019.

Zhang, T., de Jong, M. C., Wooster, M. J., Xu, W., and Wang, L.: Trends in eastern China agricultural fire emissions derived from a combination of geostationary (Himawari) and polar (VIIRS) orbiter fire radiative power products, Atmos. Chem. Phys., 20, 10687–10705, https://doi.org/10.5194/acp-20-10687-2020, 2020.

Zhao, H. M., Yang, G. Y., Tong, D. Q., Zhang, X. L., Xiu, A. J., and Zhang, S. C.: Interannual and seasonal variability of greenhouse gases and aerosol emissions from biomass burning in Northeastern China constrained by satellite observations, Remote Sens., 13, 1005, https://doi.org/10.3390/rs13051005, 2021.

Zheng, B., Ciais, P., Chevallier, F., Yang, H., Canadell, J. G., Chen, Y., van der Velde, I. R., Aben, I., Chuvieco, E., Davis, S. J., Deeter, M., Hong, C. P., Kong, Y. W., Li, H. Y., Li, H., Lin, X., He, K. B., and Zhang, Q.: Record-high CO_2 emissions from boreal fires in 2021, Science, 379, 912–917, https://doi.org/10.1126/science.ade0805, 2023.

Zhou, Y., Xia, X. C., Lang, J. L., Zhao, B. B., Chen, D. S., Mao, S. S., Zhang, Y. Y., Liu, J., and Li, J.: A coupled framework for estimating pollutant emissions from open burning of specific crop residue: A case study for wheat, Sci. Total Environ., 844, 156731, https://doi.org/10.1016/j.scitotenv.2022.156731, 2022.

Zhou, Y., Xing, X., Lang, J., Chen, D., Cheng, S., Wei, L., Wei, X., and Liu, C.: A comprehensive biomass burning emission inventory with high spatial and temporal resolution in China, Atmos. Chem. Phys., 17, 2839–2864, https://doi.org/10.5194/acp-17-2839-2017, 2017.

Zhuang, Y., Li, R. Y., Yang, H., Chen, D. L., Chen, Z. Y., Gao, B. B., and He, B.: Understanding temporal and spatial distribution of crop residue burning in China from 2003 to 2017 using MODIS data, Remote Sens., 10, 390, https://doi.org/10.3390/rs10030390, 2018.

Zhu, C., Kawamura, K., and Kunwar, B.: Effect of biomass burning over the western North Pacific Rim: wintertime maxima of anhydrosugars in ambient aerosols from Okinawa, Atmos. Chem. Phys., 15, 1959–1973, https://doi.org/10.5194/acp-15-1959-2015, 2015.